https://doi.org/10.31351/vol33iss3pp171-186

Curcumin-Loaded Organogel for The Topical Skin Disorder Based on 12 Hydroxystearic Acid

Duaa Razzaq Jaafer*,[1] and Masar Basim Mohsin Mohamed[1]

[1]Department of Pharmaceutics, College of Pharmacy, Mustansiriyah University, Baghdad, Iraq.

***Corresponding author**

Received 4/7/2023, Accepted 11/10/2023, Published 15/9/2024

Abstract

Curcumin (CUR) possesses various pharmacological properties, including antibacterial and improving injury healing. This work aimed to formulate curcumin organogel using 12 hydroxy stearic acid as gelator with tween 80 as surfactant and PEG 400 as co surfactant to improve the CUR permeation through the skin. The CUR organogels were prepared using different 12HSA concentrations with solvents sesame oil (SO), and orange oil (OO), in addition to T80 and P400 and evaluated for their saturated solubility, tabletop rheology, oil binding capacity, pH, spreadability, *in vitro* release, antibacterial activity, oscillatory rheology study, skin irritation, histological examination and *ex-* with *in- vivo* permeation study across rat abdominal skin. Results: The important results that distinguished organogels were the spreadability and *in vitro* release studies. The 4SO, 2OO, 2T80, and 10P400 organogels presented successful gelation and represented the lowest 12HSA concentration in each solvent that approached the current aim's study by being more spreadable with higher CUR released. At the same time, the 2T80 and 10P400 gave zones of inhibition to 4 bacterial strains and good viscoelasticity by exhibiting large flow point values in the frequency sweep study compared with 4SO and 2OO. *In vivo* study affirmed the CUR permeation by studying the fluorescent images of 2T80 and 10P400, and the *ex vivo* permeation study for 10P400 proved the CUR permeation through rat's skinOur results indicated the potential of 10P400 and 2T80 organogel to improve the topical therapeutic efficacy of CUR.

Keywords: Curcumin, 12-hydroxystearic acid, Organogel, Tween 80, Polyethylene glycol 400, Fluorescent intensity.

جل عضوي محمّل بالكركمين لاضطراب الجلد الموضعي أساسه حمض الهيدروكسيستريك

دعاء رزاق جعفر*،[1] و مسار باسم محسن[1]

[1]فرع الصيدلانيات ، كلية الصيدلة ، الجامعة المستنصرية ، بغداد ، العراق

الخلاصة

يمتلك الكركمين (CUR) خصائص دوائية متنوعة، بما في ذلك الخصائص المضادة للبكتيريا وتحسين الشفاء من الإصابات. هدف هذا العمل هو تحضير جل عضوي باستخدام مركب حامل الهلام ١٢-هيدروكسي ستياريك (HSA١٢) و، لأول مرة، استخدام مذيبات مادة مُسَطِّحَة "توين ٨٠" (T80) ومادة مُساعِدَة "بولي إيثيلين جلايكول ٤٠٠" (P400) كخزان للكركمين (CUR) لتحسين نفاذية الكركمين من خلال الجلد. الطريقة: تم تحضير الجل العضوي باستخدام تراكيز مختلفة من 12HSA مع CUR مع المذيبات زيت السمسم (SO) ، وزيت البرتقال (OO) ، بالإضافة إلى T80 و P400 وتم تقييم قابليتها للذوبان المشبعة ، وريولوجيا الطاولة ، وقدرة ربط الزيت ، ودرجة الحموضة ، وقابلية الانتشار ، التحرر في المختبر ، النشاط المضاد للبكتيريا ، دراسة الريولوجيا التذبذبية ، تهيج الجلد ، الفحص النسيجي ودراسة التخلل خارج الجسم الحي عبر جلد بطن الجرذ. كانت النتائج المهمة التي تميز بها الجل العضوي هي دراسات القابلية للانتشار والتحرر في المختبر. قدموا التكوير الناجح وأقل تركيز لـ 12 HSAفي كل مذيب 4SO، 2OO، 2T80 ، 10P400. لمقاربة دراسة الهدف الحالي من خلال كونها أكثر انتشارًا مع إطلاق CUR أعلى. في نفس الوقت ، أعطى T80 2و 10P400مناطق تثبيط لـ ٤ سلالات بكتيرية ومرونة لزوجة جيدة من خلال إظهار قيم نقطة تدفق كبيرة في دراسة اكتساح التردد مقارنة بـ 4SOو 2OO.أكدت دراسة في الجسم الحي تغلغل CUR من خلال دراسة الصور الفلورية 2T80و 10P400 ، وأثبتت دراسة التخلل خارج الجسم الحي لـ 10P400تغلغل CUR من خلال جلد الفئران. الاستنتاج: أشارت نتائجنا إلى إمكانات 10P400و 2 T80العضوي لتحسين الفعالية العلاجية الموضعية لـCUR .

الكلمات المفتاحية: الكركمين ، حمض ١٢ هيدروكسيستريك ، جل عضوي ، توين ٨٠ ، بولي إيثيلين جلايكول ٤٠٠ ، كثافة الفلورسنت.

Introduction

Studies on curcumin (CUR) demonstrated a wide variety of biological properties, including antioxidant , anti – inflammatory , antitumor, anti – bacterial and antiparasitic effects as well as treating skin problems and wounds (1-6). However, many studies investigated CUR for topical application

and focused on CUR solubility enhancement to increase permeation. To demonstrate, CUR-loaded nanosponge in the gel for psoriasis treatment [7]. Also, CUR-loaded nano lipid carriers for enhanced skin delivery [8]. Further, in a different study, the nanocrystal of CUR was formulated in the gel to increase CUR solubility [9]. Vigato's co-workers prepared CUR in polymeric organogel using poloxamer for topical administration [10]. CUR physicochemical properties, such as low aqueous solubility and oral bioavailability, limit CUR action [11]. Thus, these obstacles made CUR an intriguing molecule for cutaneous application [12], as this route offered the advantage of delivering the drug molecule through the skin of many topical dosage forms, such as in gels [13]. Gels formulation is an easy preparation procedure, and the polarity of the solvent or the continuous phase used to create the gel determines the classification of the gel, which can be either hydrogel or organogel [14]. The gelators of organogel represent the solid part of the gel network are either low molecular weight gelators, such as sorbitan mono palmitate, sorbitan mono stearate, and glyceryl fatty acid esters, or of a large molecule polymeric organic gelators with high molecular weight gelators [15, 16]. The current study focused on organogel using the low molecular weight gelator, the 12-hydroxystearic acid (12HSA), with a surfactant and co-surfactant, which were tween 80 (T80) and PEG 400 (P400) as an external phase or the liquid organogel's part. The selection of these liquids depended on a previous study that showed CUR high solubility in T80 and P400 [17]. This current study also included the 12HSA formulated with sesame oil (SO) and orange oil (OO) for their notable property in treating bacterial skin diseases [18, 19] . As a continuous phase of 12HSA organogel, these solvents incorporated CUR, and according to our knowledge, no previous work presented an investigation of the gelation capability of 12HSA to the T80 and P400. Considering the proposed solvents and the 12HSA, this work aimed to explore CUR organogel for local topical antibacterial and transdermal applications.

Materials and Methods

Materials

Curcumin and 12HSA were purchased from BiDePharma Technology / China and Hangzhou Hyper Chemicals/ China, respectively. Both T80 and P400 were bought from Sigma-Aldrich. SO was pur-chased from Xi'an Sonwu Biotech, China, while OO was obtained from (Now Essential Oil).

Methods

Saturated solubility of CUR

An excess amount of CUR was added to a glass vial with a stopper filled with 4 mL of the following: SO, OO, T80, P400, and phosphate buffer pH 7.4 made with 10% w/v T80. The glass vials were left in a shaking water bath (50 rpm) at 37°C for 3 days. After that, the vials were subjected to centrifugation at 3500 rpm for 30 minutes, as the supernatant was filtered using a syringe filter with a pore size of 0.45 micrometers, following this the filtrate of CUR in (SO, OO, T80, P400) was appropriately diluted with ethanol to be measured by a spectrophotometer to determine its absorbance using (UV-1650PC) Shimadzu -Japan at the λ max 425 nm using the calibration curve equation (y=136.5x+0.0087) with R2=0.9993 in ethanol , while filtrate of CUR in phosphate buffer pH 7.4 diluted with the same buffer using the calibration curve equation of (y=161x+0.016) showing R^2=0.9986 [20].

Preparation of organogel

The blank organogel was made by first weighing 12HSA in the vials and then bringing the total mass up to 1 g by adding individually SO, OO, T80 and P400. Vials were incubated in a water bath at 85°C for 10 minutes until a clear solution was obtained, and then vials were cooled at room temperature after bringing vials out of the water bath. The vials were subjected to inversion; if there were no flow of the organogels, the result would be a solid organogel; nevertheless, if there were flow when the organogels overturned, then the result would be a liquid organogel. Last, a 5 % w/w CUR organogel preparation was by using the same concentration by Jamali et al study prepared CUR ointment for topical use, followed the steps outlined above, and we mixed 50 mg of CUR combined with the 12HSA [21]; then, the mixture was heated to 85°C, where the contents were dissolved and dispersed in the solvents as shown in Table (1).

Table 1. The compositions of the CUR organogels.

Formulation name	CUR (mg)	12HSA% (w/w)	Oil Up to 1gm
0.5SO	50	0.5	SO
1SO	50	1	SO
2SO	50	2	SO
3SO	50	3	SO
4SO	50	4	SO
5SO	50	5	SO
6SO	50	6	SO

Continued Table 1.

0.5OO	50	0.5	OO
1OO	50	1	OO
2OO	50	2	OO
3OO	50	3	OO
4OO	50	4	OO
0.5T80	50	0.5	T80
1T80	50	1	T80
2T80	50	2	T80
3T80	50	3	T80
4T80	50	4	T80
0.5P400	50	0.5	P400
1P400	50	1	P400
2P400	50	2	P400
4P400	50	4	P400
6P400	50	6	P400
8P400	50	8	P400
10P400	50	10	P400
11P400	50	11	P400
12P400	50	12	P400

Tabletop rheology (Transitions temperature)

The CUR organogels vials were placed in a water bath and heated to 85°C. Afterwards, the temper-ature drop was 2°C every 15 minutes until 32 °C. At the end of each 15 minutes, the vials were tilted to determine if the organogel formulation was liquid or solid. In this phase, the solidifying points of all organogels were determined; subsequently, the vials entered another stage. The temperature was increased by 2 °C every 15 minutes until 85 °C record the melting points[22].

Oil binding capacity (OBC)

Vial containing 1g of CUR organogel was centrifuged for 15 minutes at 6000 rpm. The vial was inverted over the filter paper for 5 minutes to collect the free liquid oil dropping from the organogel. The quantity of oil expressed was then determined by weighing the filter paper, as this study was done in triplicate. To calculate OBC(%), use the equation (1) [23].

$$\boldsymbol{OBC}\% = \left(\mathbf{1} - \frac{\boldsymbol{mass\ of\ expressed\ oil}}{\boldsymbol{initial\ sample\ mass}}\right) \times \mathbf{100} \qquad \textbf{(1)}$$

pH determination

The pH for all CUR organogels was measured by putting a digital pH meter probe into the organogels and monitoring the readings until equilibrium was reached [10].

Spreadability

The organogel ability to spread was by placing 0.5 grams of the prepared CUR organogel within a circle with a diameter of 1 centimeter (cm) on a glass slide. Next, a second glass slide was placed over the first with the exact dimensions, sandwiching the gel between the upper and lower glass slides. After 5 minutes of rest and by the placing weight of 5 g, the sandwiched organogel between the two glass slides would be forced to squeeze and spread, and the increase in organogel spreading diameter was measured [24].

In vitro release study

A dissolution apparatus was set at a paddle speed of 50 rpm using a modified form of Franz cell by a glass cup with a cross-sectional area of 2 cm2, filled with 1 g of the CUR organogels, covered with a cellulose membrane(0.45µm) and sealed with a rubber band. Then cup inversion ensured the membrane levelled by 0.5 mm under the surface of 50 mL phosphate buffer using pH 7.4, as in both studies of diclofenac formulations and CUR nanoparticles for topical *in vitro* release [25, 26]. Also, the prepared 50 ml phosphate buffer pH 7.4 with 10% w/v T80 at 37 °C was added to ensure the sink condition; Shahani *et al* found that CUR was more soluble at pH 7.4 with 10% T80 [27]. For 24 hours, aliquots of 5ml were removed within predetermined intervals and promptly replaced with a fresh buffer medium after each removal. A UV-VIS spectrophotometer was used to perform spectrophotometric analysis at 425 nm to assess the CUR amount using the equation that was clarified in the saturated solubility study [28].

Antibacterial activity

The agar well diffusion method was used to investigate the antibacterial activity of selected CUR organogels against four clinically isolated strains of bacteria*: Staphylococcus aureus*, *Streptococcus pyrogen*, *Proteus mirabilis*, and *Escherichia coli*. The prepared agar was inoculated with a sterile glass spreader to disseminate a 0.1 mL bacterial suspension. The wells were constructed having a diameter of 6 mm in each plate, and 50 µl of carefully chosen CUR liquid organogels were deposited; the SO, OO, T80 and P400 were also used as controls containing CUR 5 % w/w. Then the

plates were rested at ambient temperature then placed in an incubator at 37 ºC for 24 hour [29, 30]. The inhibition zone was measured and given in millimeters [31].

Oscillatory rheology studies

Rheology studies on selected CUR organogels were conducted using Anton par mcr 302 rheometer (Graz, Austria) and a plate-plate (PP 25/ SN 61895) was utilized. At 25°C, each measurement was performed in triplicate, and Rheoplus software was used for data extracting [32]. These examinations of CUR-loaded organogel were conducted at the University of Petra and the Pharmaceutical Center in Amman, Jordan. For amplitude and frequency sweep tests, a scoop of selected organogel was placed between the two plates (PP 25/ SN 61895).

a) *Amplitude sweep*

Initially, to start rheology studies by performing amplitude sweep test. The purpose of this test was to identify the storage modulus (G'), the loss modulus (G''), the flow point for each formulation, and the linear viscoelastic area (LVER). Hence, the oscillatory strain range was varied from 0% to 100%, and the angular frequency was kept constant at 10 rad s^{-1}.

b) *Frequency sweep*

The second oscillatory test was the frequency sweep, and the strain applied was between 0.01% and 0.08%, according to the LVER data obtained from the amplitude sweep test data for each organo-gel. The angular frequency varied from 0.1 to 100 rad s^{-1} during this test.

Skin Irritation Studies

Healthy male Wister Albino rats aged 2-3 months weighing 250–350 g were used to investigate skin irritation. A day before the appointed experiment, the hairs on the abdomen of each rat were carefully shaved with an electrical clipper without damaging the stratum corneum. The area of application was swept with dried cotton. The Draize patch test was utilized in investigations of skin irritation. Five groups (gp), each of 1 rat, classified to gp A: treated with 4SO, gp B: treated with 2OO, gp C: treated with 2T80, gp D: treated with 10P400, and the last was gp E: treated with 0.8% v/v aqueous solution of formalin (which is a standard irritant). The cutaneous irritation work was conducted for 3 days [33]. The severity of cutaneous irritation was evaluated by the visual scoring scale of 0, 1, 2, 3 and 4, indicating no skin irritation, minor skin irritation, well-defined skin irritation, moderate-level skin irritation and scarring on the skin, respectively [34].

Histological examination of organogel-treated skin

This test followed the irritancy test to study the possible changes in skin histology after applying selected CUR organogels; additionally, another rat was chosen as a control without any treatment or addition the techniques involved cross sectioned and dyeing the skin after the rats were sacrificed. Then, rat skin samples were embedded in paraffin wax blocks and submitted to electrical microtomy to be cross-sectioned into thin slices measuring 5µm. After being cut into cross-sections, these skin samples were stained with hematoxylin and eosin (H&E) dyes to be analyzed using a microscope [35].

In vivo CUR permeation study

CUR penetration through the skin was executed by applying the organogels to the rat's abdominal area following the same irritancy test and histological procedures. This test needed 3 rats for each selected formulation, as each rat was sacrificed after 1, 4, and 24 hours of CUR organogel application. Then, the skin sectioning for microscopic slide preparation proceeded with gentle and prolonged water rinsing to remove the applied organogel. The prepared slides were studied optically using the z-axis of an inverted trinocular LED fluorescence microscope (OPTIKA microscopy, Italy) equipped with the Optica camera and software for imaging, as the procedure was performed in the darkroom to avoid the impact of ambient light using the blue field filter that is suitable for the CUR excitation wavelength of 425 nm and emission wavelength of 515 nm [36, 37]. The level of microscope light intensity was at 5, which was applied while inspecting the slides and imaging. The microscope magnification power was 10x. The fluorescent intensity was determined using the acquired images and ImageJ software (a Fiji distribution dedicated to biological image analysis). Each image was counted as a single fluorescent intensity unit. We autonomously analyzed the pixel intensity for each image using an 8-bit image histogram. Upon completion of the histogram analysis, the parameters mean gray value (MGV) and standard deviation are determined to investigate the fluorescent intensity that correlates with CUR penetration [38].

Ex Vivo CUR Permeation Study

Ex vivo permeation through the excised abdominal skin of male Wister Albino male rats was evaluated by utilizing a Franz diffusion cell with the exact dimensions used in the *in vitro* release study. The excised skin was put over the recipient compartment (2 cm^2) with the epidermal side of the skin exposed to ambient conditions, while the dermal side was kept facing the receptor solution, as the receptor compartment was filled with phosphate buffer solution pH 7.4 + 10% w/v T80 and the temperature was kept at 37 ±0.5 °C [17]. At specified time intervals of (0.1, 0.5, 1, 2, 4, 8, 12, 18, 20, and 24) hours, 2 ml samples of the receptor medium were withdrawn, and immediately fresh phosphate buffer solution was added to maintain the sink condition [39]. The samples were analyzed by the HPLC modified method following the Hiserodt *et al* method [40]. The curcumin content was analyzed

using an HPLC system consisting of a Shimadzu HPLC LC-10AT pump. A 25-cm long, 4.6-mm inner diameter of the C18 column (LichroCart 250-4, Merck) was used. The mobile phase consisted of a 50% aqueous phase which was water adjusted to pH 7.4 with acetic acid 2 wt.% and 50% acetonitrile, with a 1.7 ml/ min flow rate. The wavelength of the fluorescence detector was set at an excitation of 425 nm and an emission of 515 nm [36, 37].

Results and discussion

Saturated solubility of CUR

The saturated solubility of CUR was determined to evaluate the solubility of CUR in oils, surfactant, cosurfactant and buffer, which may play a role in CUR release from organogels, specifically oils, and ensuring the sink condition for CUR in the buffer. The solubility was 1.011, 0.905, 34.38, 35.43 and 1.8 mg/ml, in SO, OO, T80, P400 and phosphate buffer 7.4 + 10% w/v T80, respectively. Fairly similar values of the CUR saturated solubility in SO, OO, T80, and P400 were to the previous study [41]. CUR showed the lowest solubility in OO, and CUR was more highly soluble in P400 than in T80 and SO.

Interestingly, the phosphate buffer with a pH of 7.4 + 10% w/v T80 had the lowest value of CUR solubility. This result predicted that the CUR prepared with organogel was more soluble than the CUR released through *in vitro* release study.

Preparation of organogel

Oragnogel formulations that were solid and did not flow after flipping the vials at room temperature assisted in determining the minimum gelation concentration of 12HSA in each selected solvent. Figure (1) shows the minimum gelation concentration was 4 % w/w, 2 % w/w, 2 % w/w and 10 % w/w for the SO, OO, T80 and P400, respectively. These differences in the minimum gelation concentration might be attributed to the different solubility of 12HSA in the solvents, whether these solvents were oils, surfactants, or co-solvents. After that, the CUR addition to each solvent started from the minimum gelation concentration of 12HSA that gelled the solvents with the other 2 concentrations, as shown in Table (2), as CUR addition did not affect the organogel formation.

Tabletop rheology (Transition temperature)

Tabletop rheology is a procedure that describes the phase transitions from gel to sol (T gel-sol) and from sol to gel (T sol-gel) for thermosensitive organogels. As the transition temperature is higher than the body temperature, the organogel can maintain its solid state. The temperatures at which the phase change from gel to sol and vice versa are listed in Table (3). The value (Tsol-gel) that was recorded to be the greatest was for 4SO, while the value that was reported to be the lowest was for 12P400. Previous research that combined 12HSA with light mineral oil yielded findings comparable to those obtained with 12HSA organogel in this experiment [42]. In conclusion, the temperatures at which the curcumin organogels transitioned from solid to liquid states were higher than the average body temperature. This ensured that the organogels remained solid on the skin.

Oil binding capacity (OBC)

Since the strength of the scaffold that builds an organogel and holds the oil is reflected in the organogels binding capacity [43]. Table (3) shows that the OBC of organogels in T80 was considerably lower than the organogels in SO, OO, and P400. Furthermore, the concentration of organogels was directly correlated with the OBC, which might indicate concentrated organogels entrapped the solvents strongly. This is similar to the trend of folic acid in propylene glycol organogel upon an increase folic acid concentration [44].

pH determination

Due to the topical application of organogel on the skin, pH measurements were carried out since non-suitable pH could irritate the skin [10]. As seen in Table (3), the pH levels of CUR organogels ranged from 4.43 to 5.83. These findings were consistent with the previous studies of the CUR pluronic lecithin organogels that indicated no potential for skin irritation as the organogel's pH range (4 -6) was compatible with the skin pH (slightly acidic), reflecting no risk of skin irritation [45].

Spreadability

This test demonstrated the skin preparation's capacity to distribute topically upon application, contributing to the formulation's therapeutic efficacy. In addition, this is considered a significant element in the patient's compliance with the treatment [46]. The test for spreadability was performed on all of the CUR organogels, and the results are presented in Table (3). The diameters of the spread circles vary from 1.3 cm for 6SO organogel and up to 3 cm for 2T80 organogel.

According to our results, the organogels with the lowest 12HSA concentration in each solvent, specifically 4SO, 2OO, 2T80, and 10P400, were the most easily spreadable.

Table 2. The organogel names and minimum gelation concentrations as 5 wt % CUR was in each organogel.

Organogel	12HSA wt%	Oil (up to 1g)
4SO	4	SO
5SO	5	SO
6SO	6	SO
2OO	2	OO
3OO	3	OO
4OO	4	OO
2T80	2	T80
3T80	3	T80
4T80	4	T80
10P400	10	P400
11P400	11	P400
12P400	12	P400

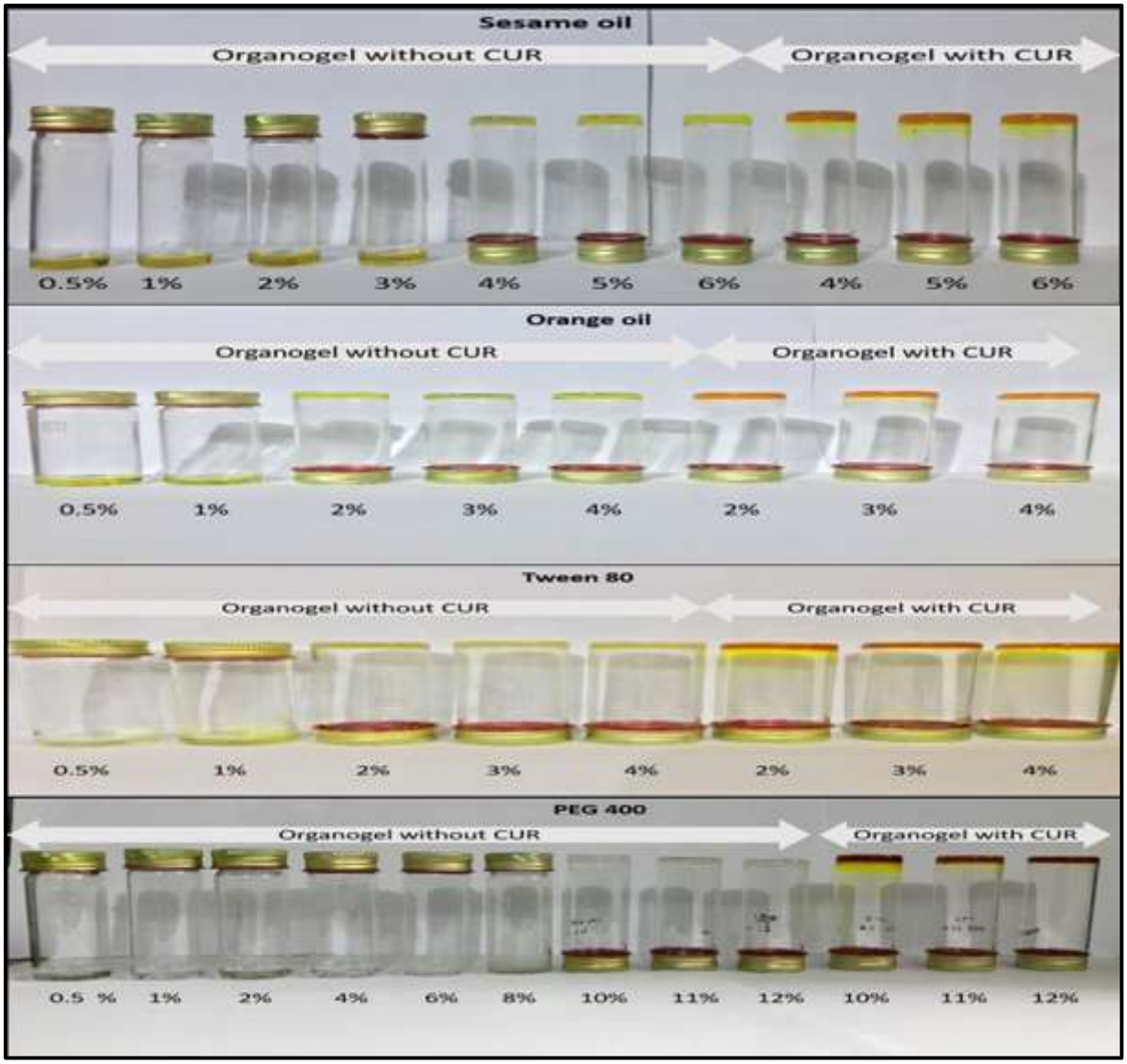

Figure 1. Organogels of 12HSA in SO, OO, T80 and P400 as the inverted vials referred to as solid organogel at room temperature for Organogel without CUR. The last 3 vials represented the CUR organogel, as pointed out in each image. All prepared organogel as % w/w.

Table 3. The tabulated results present the Tsol-gel, Tgel-sol, OBC%, pH and spreadability results for CUR organogel.

Organogel	(Tsol-gel) °C	(Tgel-sol) °C	OBC % ±SD	pH	Spreadability in cm
4SO	32.5	39.1	95.7±1.23	4.85	1.75
5SO	31.2	39.7	96.9±0.34	4.75	1.5
6SO	29.8	40.2	98.8±0.52	4.43	1.3
2OO	30.3	39	53±3.21	5.71	1.8
3OO	29.6	39.4	91.5±2.95	5.52	1.65
4OO	29.1	39.5	96.2±0.25	5.83	1.5
2T80	30.7	39.2	26.9±0.61	5.27	3
3T80	30.3	39.7	48.5±3.14	5.31	2.8
4T80	29.4	41	69.9±2.33	5.35	2.6
10P400	27.7	42.3	56.4±1.61	5.12	1.85
11P400	27.3	43	63.9±0.33	5.23	1.65
12P400	26.2	43.7	78.8±3.16	5.41	1.5

In vitro release study

In order to evaluate the CUR release from the organogels or the depot feature of organogels, *in vitro* release study was conducted using CUR organogels for 24 hours. As can be seen in Figure (2), control was run alongside the release investigations composed of 50 mg CUR mixed individually in SO, OO, T80, and P400 to compare with the corresponding organogels. These controls were established due to the oil's well-documented capacity to reduce the release rate of lipophilic drugs [47].

The results demonstrated an indirect relationship between the organogel concentration and the amount of released CUR, as the highest amount of CUR was released from the lower concentration of 12HSA organogels in each solvent. The same trend was established in a different study using 12HSA/SO organogel in which the amount of released cinnarizine was reduced with a greater organogel concentration [48]

The organogel 2T80, as shown in Figure (2), exhibited a rapid CUR release and reached 100 % w/w of CUR in the release medium within 6 hours. On the other hand, the organogels of 3T80, 4T80 released CUR at approximately 87 and 73 (% w/w), respectively. Nevertheless, the in vitro release study for the other CUR organogels in OO, SO and P400 were conducted for 24 hours. The organogels 5SO and 6SO exhibited closed release profiles, as shown in Figure (2), and within 24 hours, they released 20 % w/w CUR. However, 4SO had a significantly higher CUR release during the study, about 70 % w/w.

The 2OO and 3OO both released 40 % w/w CUR after 24 hours. As can be seen in Figure (2), the released CUR profiles for 10P400, 11P400, and 12P400 in the final set of organogels containing 12HSA in P400 were extremely asymptotic, and the alterations that occurred were not particularly substantial.

The differences in the release profiles could be attributed to several factors, including CUR solubility in solvents (the external phase of the organogel) and the organogel strength, as demonstrated by the OBC study. For example, the organogel of 2T80 that released 100 % w/w CUR within 6 hours showed the lowest value of OBC, which was 26 % w/w might aid the rapid CUR migration from the scaffold of the organogel.

However, the P400 organogels and despite the high solubility of CUR in P400, the CUR was able to be held and released gradually. This might be due to the high gelator concentration of 12HSA, as the minimum gelation concentration required was 10 % w/w.

It can be stated that all CUR organogels slowed the release of CUR by varying percentages compared with their control, demonstrating the importance of organogel in maintaining the CUR inside its network. Also, as clarified in their release profiles, the T80 and P400 organogels released CUR faster than OO and SO organogels.

From spreadability results, the CUR organogels with lower concentrations were more spreadable. The *in vitro release* study showed the same trend that the organogels with the lowest concentration of 12HSA in different solvents released more CUR. Both results assisted in approaching this study's aim to increase CUR availability through the skin; hence, the following organogels, 4SO, 2OO, 2T80 and 10P400, were processed for further studies.

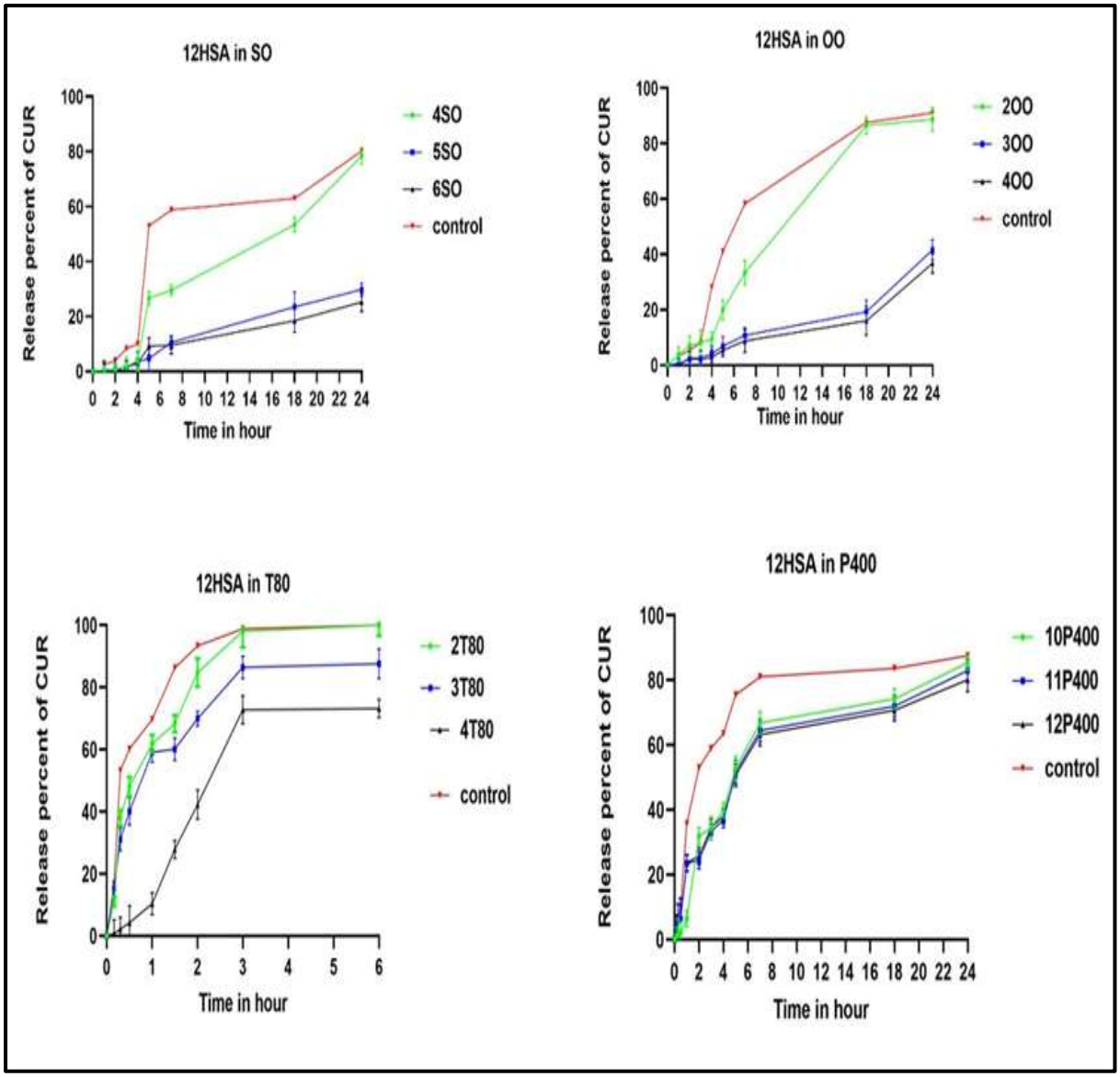

Figure 2. ***In vitro*** **CUR organogels release in pH 7.4 sodium phosphate buffer solution + 10% w/v Tween80 at 37°C. for 12HSA in SO, OO, T80, and P400, as each release curve is an average of triplicate ± standard deviation.**

Antibacterial activity

The use of CUR as an antibiotic was against the selected bacteria*: Staphylococcus, streptococcus pyrogen, Escherichia coli, and Proteus mirabilis*, as these microorganisms are capable of potentiating skin diseases. Thus, it was necessary to provide evidence that the chosen organogels could effectively cure many bacterial skin strains. The findings (not shown) presented the 4SO and 2OO could not inhibit the growth of the strains used in this study, even with CUR control. However, the 2T80 and 10P400 showed a close noticed inhibition of the zone towards the bacterial strains as their controls displayed consistently larger inhibition zones as shown in Figure 3 (A and B). This may be associated with the increased CUR availability in combat-ing bacteria to disperse their cell membrane, which might be owing to the high solubility of CUR in the surfactant T80 and co-surfactant P400, as shown in the result of saturated solubility. The most effective organogel against bacteria was 2T80, followed by 10P400. Based on this evidence, CUR has therapeutic potential for treating skin and chronic wound infections [49, 50]. Moreover, the OO and SO organogels did not give any antibacterial effect

.

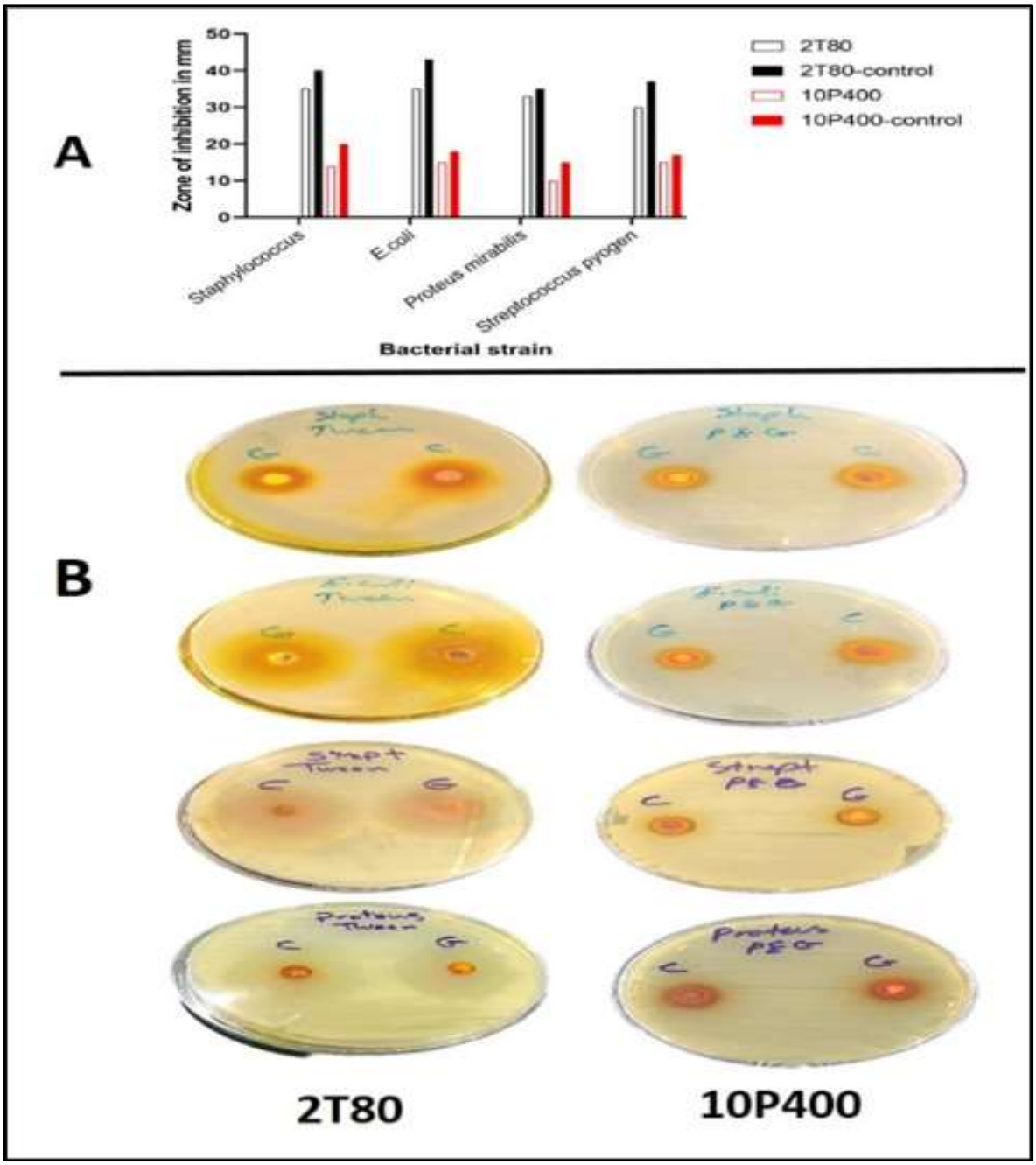

Figure 3A. Antibacterial activity of CUR showing the zone of inhibition versus bacterial strain as the bars represent the organogels that showed zone of inhibition against bacteria. 3B. the 1st, 2nd, 3rd and 4th rows show the agar results of *Staphylococcus, streptococcus pyrogen, Escherichia coli,* and *Proteus mirabilis.*

Oscillatory rheology studies

a) Amplitude sweep

This investigation used the amplitude sweep test to determine G', G", LVER, and the flow point for the chosen organogels (4SO, 2OO, 2T80, and 10P400). G', which represents the solid phase and the elastic nature of organogels whereas G" indicated the liquid phase [51]. The scooped organogel was subjected to a rising strain from 0% to 100%. If the gel proves to have good strength; in that case, G' values will be greater than G" values. This was shown by the parallel G' and G" curves and the consistent values of G' and G" until a strain value is reached that the gel cannot be as 3-dimensional scaffolds marking the start of gel weakening as observed by the LVER. At some point afterwards, the gel cracks under increasing strain value. This is the flow point, where G' and G" have identical values. The parameters are shown in Figure (4) and Table (4), used to gauge the strength of any organogel. All selected organogels showed parallel curves of G', and G" as well; the most important was that G' values in LVER were higher in the magnitude of one order than G". This

property establishes organogel formation that was indicated by Yan *et al* [52]. In addition, the extent of G' values ranged from 10^3 to 10^6, likewise the prepared organogels of 12HSA in canola oil [53].

Concerning the LVER, the 2T80 exhibited a comparable value of LVER to 0.106 of folic acid organogel in propylene glycol [44]. Different LVER values of selected organogels could be attributed to the beginning of increasing the spaces in the 3-dimensional organogels scaffold due to the rising applying strain effect. This paved to detaching of the physical bonds between constructed fibers that composed the entangled or cross-linked 3-dimensional scaffold [54]. Regarding the flow point and compared to the other organogels, 2T80 exhibited the highest value, and the 4SO showed the lowest values. The flow points represent where the organogel lost its elasticity, transferring to the liquid phase; this may be due to the complete detachment of physical bonds between fibers.

To sum up, 10P400 showed the highest values of G', and flow points, as well as 2T80 showed the high values of flow points despite the lower G' values. As the flow point explicitly represents the elasticity of organogels and the magnitude of resistance that face the increasing strain values.

b) Frequency sweep

This study was conducted to check how organogel maintained its solid form in a 3-dimensional scaffold when organogels were carried at various velocities. In most cases, the G' and G" curves for a robust organogel will not cross. As shown in Figure (4), the G' curves were higher and parallel to the G" curves of all 12HSA organogel and did not cross at any frequency rate. This means that all organogels were solid at all frequency ranges. This outcome was similar to the parallel G' and G" curves of 0.88 wt% 12HSA/ dodecane organogel [55]. To conclude, the selected organogels were frequency independent along all the studied frequency ranges.

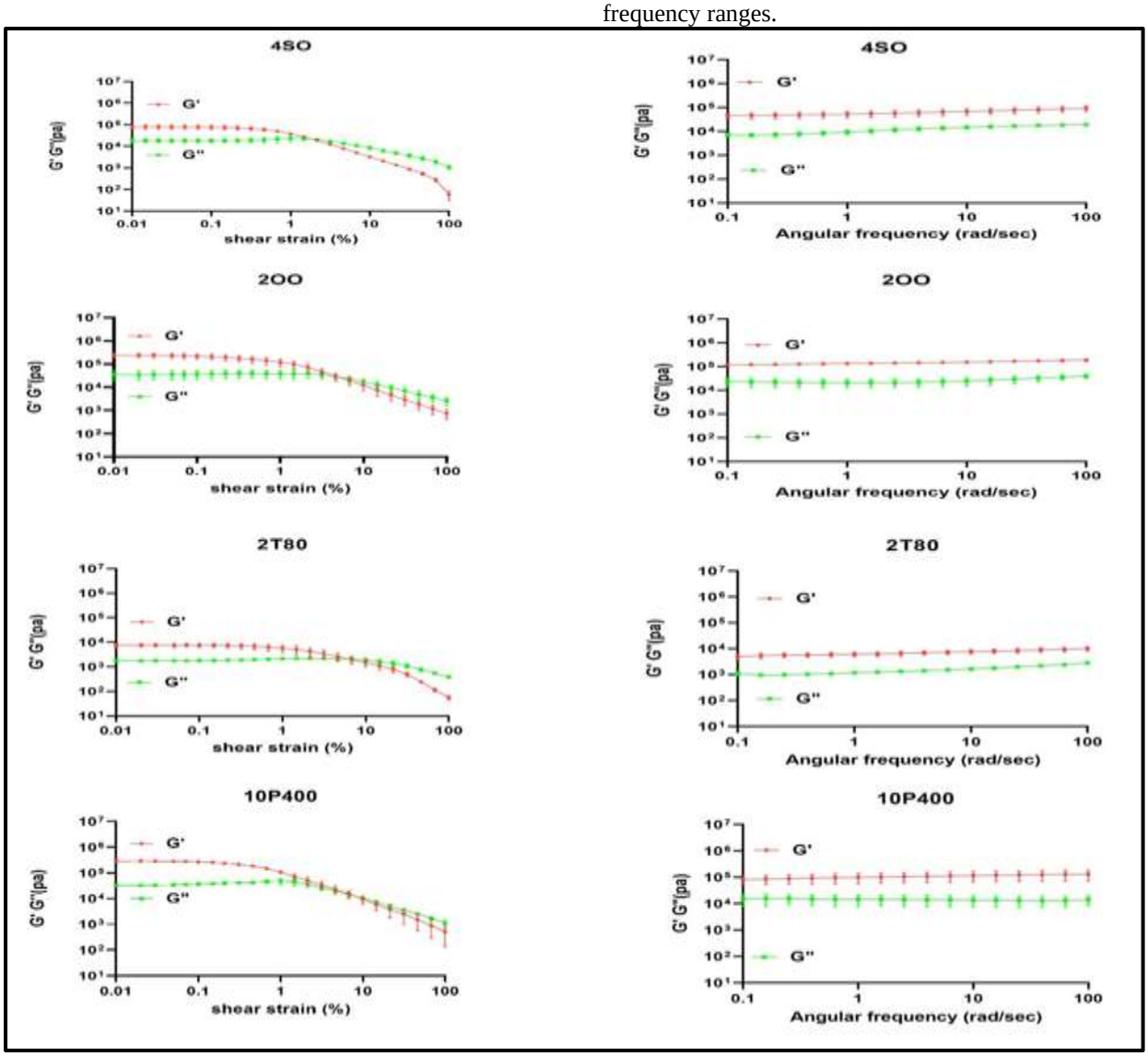

Figure 4. Rheology oscillatory Figures, the left side represents the amplitude sweep, and the right side represent the frequency sweep of the organogels of 4SO, 2OO, 2T80 and 10P400.

Table 1. Amplitude sweep parameters G', G'', LVER, and flow points for the selected organogels as each value is an average and standard deviation of 3 values. The study was set at a strain from 0% to 100%, angular frequency 10 rad.s-1, and temperature of 25°C.

Organogels	G' (pa) ±SD	G'' (pa) ±SD	LVER (%)±SD	Flow point ±SD (%)
4SO	39708 ±7444	14492 ±3007	0.088 ±0.009	2.15± 1.31
2OO	116545 ±30828	28033 ±11082	0.547±0.083	4.63 ± 0.8
2T80	7568±1225	1710 ±151	0.192 ±0.09	6.81± 1.42
10P400	134968 ±6629	26762 ±3187	0.062 ±0.043	6.78 ± 0.05

Skin irritation Studies

The skin irritation observation scores were 0 for all selected organogels. In contrast, the formalin score was 4, indicating that the organogels were non-irritant compared to formalin, which caused severe erythema and edema.

Histological examination

The studying of skin histology ensured the outcomes of the skin irritancy test. As shown in Figure (5), the histopathological images of the skin treated with selected organogels and the control skin (untreated skin with CUR organogels) exhibited a typical appearance of epidermis epithelium (keratinized stratified squamous epithelium). Also, the images showed normal dermis fibrous connective tissue composed of fibroblasts and fibrocytes, with numerous immature hair follicles and normal sebaceous glands. The histopathological photos of the skin treated with formalin exhibited marked epithelial shedding, a very thin epidermis, degenerated fibrous tissue, and regressed hair follicles. Also, the image revealed a single layer of epidermal epithelial cells that rested on a layer of degenerated fibrous tissue of the dermis composed of fibrocytes and a few regressed hair follicles. To sum up, the histology examination proved the non-irritant contents of selected organogels.

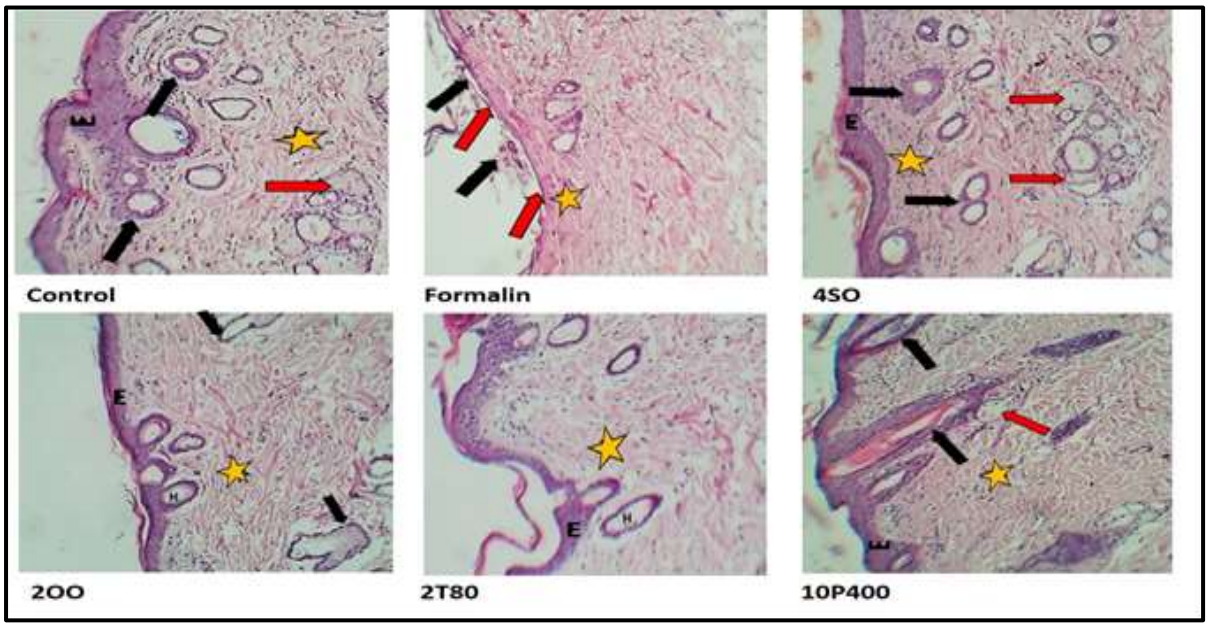

Figure 5. Microscopic images of CUR organogels, at a magnification of 100x, where epidermis (E), dermis fibrous connective tissue (Asterisk), variable stages of developing hair follicles (Black arrows) & sebaceous glands (Red arrows). Except for formalin, where marked epithelial shedding (Black arrows), very thin epidermis (Red arrows), degenerated fibrous tissue (Asterisk) & regressed hair follicle.

In vivo CUR permeation study

The remarkable outcomes of the spreadability test, frequency sweep study, and antibacterial study of the 10P400 and 2T80 organogels compared with 4SO and 2OO suggested selecting the 10P400 and 2T80 for *in vivo* CUR permeation; furthermore, by using the advantage of gaining fluorescence from CUR by absorbing and emitting light in the visible region of the spectrum and correlating the grey values of the pixels to CUR permeation through the rat's skin imaged under a fluorescence microscope. The ImageJ was used to convert the original coloured images to 8-bit images. Then the histogram analysis was used to calculate the MGV, as seen in Figure (6A)[56]; as clearly noticed sum up, the histology examination proved the non-irritant contents of selected organogels.

Which leads us to conclude that untreated rat skin has low auto fluorescence.

The MGV pattern, as shown in Figure (6B), reflecting the CUR permeation through the rat's skin was very coordinated with the *in vitro* release of both organogels, as the 10P400 MGV increased in the first hour; then, the MGV declined after 4 hours, followed by the rise in the MGV to reach 100 pixel. The decrease in MGV after 4 hours might be due to the CUR permeation out of the skin. While the 2T80 presented high and close values of MGV for both images pointed to the 1 and 4 hours, then a decrease in MGV after 24 hours. The 2T80 permeation was very high and reached 80 MGV in the first and after 4 hours due to the rapid release of CUR that penetrated quickly too. This subsequently, after 24 hours, showed depletion in the MGV, and this might be to the completed CUR release in the first 6 hours of the release study.

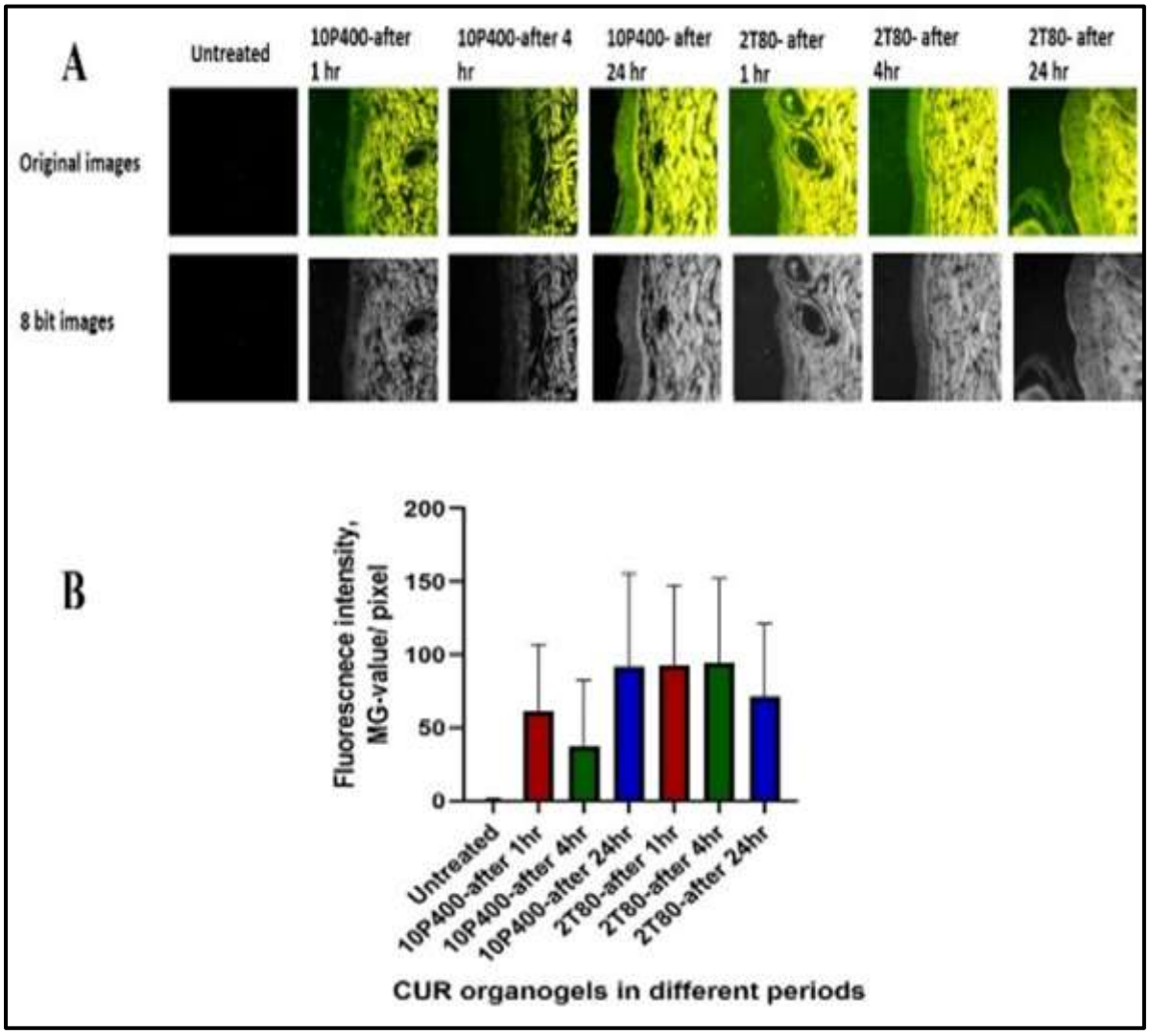

Figure 6 A. 8-bit images. B. Fluorescence intensity quantification from the 8-bit images using MGV *Ex Vivo CUR Permeation Studies*

The permeation of topical formulation through the skin is essential to affirm CUR invasion through the skin, as this was confirmed by *in vivo* CUR permeation study. The 2T80 and 10P400 showed different fluorescent intensities represented by MGV, as these fluorescence might be correlated to CUR *invitro* release study. Thus, the 10P400 was chosen to apply for this study to investigate its permeation as it showed lower MGV in the 1 and 4 hours. As shown in Figure (7), the CUR penetration was raised to 17 % w/w after 4 hour, followed by around 50 % w/w, and after 24 hour, the CUR permeation reached approximately 80 % w/w. This permeation might be attributed to the good solubility of CUR in P400. Interestingly, the amount of permeated CUR in the *ex vivo* study was 86 % w/w, which is close to the CUR released amount in the *in vitro* release study. This finding was similar to a previous study for Nawaz *et al* that formulated CUR hydrogel containing various concentrations of eucalyptus oil, aloe vera oil and clove oil using carboxy methyl cellulose (CMC) as a gelling agent,

showing a close CUR released and permeated amount[57].

This rapid CUR permeation could be justified by the P400, which proved increasing the CUR solubility as the saturated solubility in this study indicated, in addition to its known function as a permeation enhancer[58].

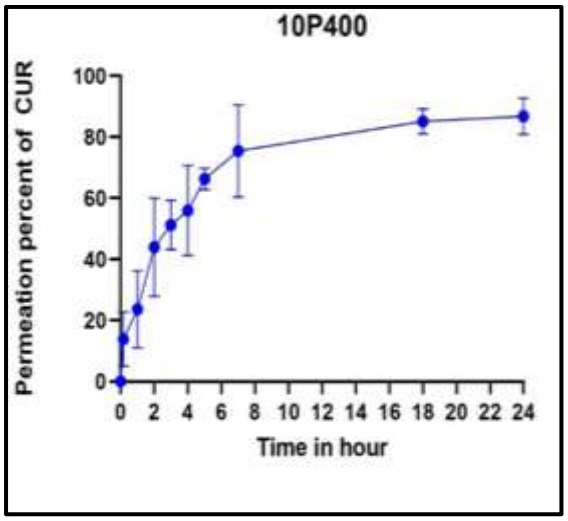

Figure 7. *Ex vivo* permeation of 10P400 organogel in phosphate buffer solution pH 7.4 + 10 %w/v T80 through Wister rat abdominal skin using Franz cell diffusion.

Conclusion

From our work, we concluded that 12HSA gave good gelation of the surfactant T80 and the co-surfactant P400 in addition to oils SO and OO. Indeed, the organogels 2T80 and 10P400, amongst other investigated organogels, achieved good antibacterial activity against specific types of bacteria and good permeation across the skin which was 86% w/w; hence, these organogels were good candidates for curcumin topical and transdermal formulation.

Acknowledgement

The authors would like to thank Mustansiriyah University (www. uomustansiriyah .edu.iq)Baghdad -Iraq and all participants for providing the practical platform of this study.

Conflicts of interest

No competing interests were disclosed.

Funding

The author declared that no grants funding our research.

Ethics Statements

This research was conducted under Medical Research Ethics Committee in the Iraqi medical research center (none profit research organization), College of Pharmacy, Mustansiriyah University, Baghdad, Iraq, ethical approval number 1\ 24-10-2022.

Author Contribution

Study conception and design: Duaa Razzaq, Masar Basim; data collection: Duaa Razzaq; analysis and interpretation of results: Duaa Razzaq, Masar Basim; draft manuscript preparation: Duaa Razzaq;supervision: Masar Basim. All authors reviewed the results and approved the final version of the manuscript

References

1. Dall'Acqua S, Stocchero M, Boschiero I, Schiavon M, Golob S, Uddin J, et al. New findings on the in vivo antioxidant activity of Curcuma longa extract by an integrated 1H NMR and HPLC–MS metabolomic approach. Fitoterapia. 2016;109:125-31.
2. Zhu H, Xu T, Qiu C, Wu B, Zhang Y, Chen L, et al. Synthesis and optimization of novel allylated mono-carbonyl analogs of curcumin (MACs) act as potent anti-inflammatory agents against LPS-induced acute lung injury (ALI) in rats. European Journal of Medicinal Chemistry. 2016;121:181-93.
3. Han Y-M, Shin D-S, Lee Y-J, Ismail IA, Hong S-H, Han DC, et al. 2-Hydroxycurcuminoid induces apoptosis of human tumor cells through the reactive oxygen species–mitochondria pathway. Bioorganic & medicinal chemistry letters. 2011;21(2):747-51.
4. Cetin-Karaca H, Newman MC. Antimicrobial efficacy of plant phenolic compounds against Salmonella and Escherichia Coli. Food bioscience. 2015;11:8-16.
5. Morais ER, Oliveira KC, Magalhães LG, Moreira ÉB, Verjovski-Almeida S, Rodrigues V. Effects of curcumin on the parasite Schistosoma mansoni: a transcriptomic approach. Molecular and biochemical parasitology. 2013;187(2):91-7.
6. Patel NA, Patel NJ, Patel RP. Design and evaluation of transdermal drug delivery system for curcumin as an anti-inflammatory drug. Drug development and industrial pharmacy. 2009;35(2):234-42.
7. Iriventi P, Gupta NV, Osmani RAM, Balamuralidhara V. Design & development of nanosponge loaded topical gel of curcumin and caffeine mixture for augmented treatment of psoriasis. DARU Journal of Pharmaceutical Sciences. 2020;28:489-506.
8. Rapalli VK, Kaul V, Waghule T, Gorantla S, Sharma S, Roy A, et al. Curcumin loaded nanostructured lipid carriers for enhanced skin retained topical delivery: optimization, scale-up, in-vitro characterization and assessment of ex-vivo skin deposition. European Journal of Pharmaceutical Sciences. 2020;152:105438.

9. Kotian V, Koland M, Mutalik S. Nanocrystal-Based Topical Gels for Improving Wound Healing Efficacy of Curcumin. Crystals. 2022;12(11):1565.

10. Vigato AA, Querobino SM, De Faria NC, Candido ACBB, Magalhães LG, Cereda CMS, et al. Physico-chemical characterization and biopharmaceutical evaluation of lipid-poloxamer-based organogels for curcumin skin delivery. Frontiers in Pharmacology. 2019;10:1006.

11. Priyadarsini KI. The chemistry of curcumin: from extraction to therapeutic agent. Molecules. 2014;19(12):20091-112.

12. Anand P, Thomas SG, Kunnumakkara AB, Sundaram C, Harikumar KB, Sung B, et al. Biological activities of curcumin and its analogues (Congeners) made by man and Mother Nature. Biochemical pharmacology. 2008;76(11):1590-611.

13. Gholibegloo E, Mortezazadeh T, Salehian F, Ramazani A, Amanlou M, Khoobi M. Improved curcumin loading, release, solubility and toxicity by tuning the molar ratio of cross-linker to β-cyclodextrin. Carbohydrate polymers. 2019;213:70-8.

14. Roy SG, De P. Swelling properties of amino acid containing cross-linked polymeric organogels and their respective polyelectrolytic hydrogels with pH and salt responsive property. Polymer. 2014;55(21):5425-34.

15. Esposito CL, Kirilov P, Roullin VG. Organogels, promising drug delivery systems: An update of state-of-the-art and recent applications. Journal of controlled release. 2018;271:1-20.

16. Kaddoori ZS, Mohamed MBM, Kadhum WR, Numan NA. To Consider The Organogel Of Span 40 And Span 60 In Sesame Oil As A New Member In The Gastro Retentive Drug Delivery Systems. Systematic Reviews in Pharmacy. 2020;11(5):850-61.

17. Thomas L, Zakir F, Mirza MA, Anwer MK, Ahmad FJ, Iqbal Z. Development of Curcumin loaded chitosan polymer based nanoemulsion gel: In vitro, ex vivo evaluation and in vivo wound healing studies. International journal of biological macromolecules. 2017;101:569-79.

18. Sun P, Zhao L, Zhang N, Wang C, Wu W, Mehmood A, et al. Essential oil and juice from bergamot and sweet orange improve acne vulgaris caused by excessive androgen secretion. Mediators of Inflammation. 2020;2020.

19. Wei P, Zhao F, Wang Z, Wang Q, Chai X, Hou G, et al. Sesame (sesamum indicum l.): A comprehensive review of nutritional value, phytochemical composition, health benefits, development of food, and industrial applications. Nutrients. 2022;14(19):4079.

20. 20. Kumar L, Suhas B, Pai GK, Verma R. Determination of saturated solubility of naproxen using UV visible spectrophotometer. Research Journal of Pharmacy and Technology. 2015;8(7):825-8.

21. Jamali N, Adib-Hajbaghery M, Soleimani A. The effect of curcumin ointment on knee pain in older adults with osteoarthritis: a randomized placebo trial. BMC Complementary Medicine and Therapies. 2020;20(1):1-10.

22. Raghavan SR, Cipriano BH. Gel formation: phase diagrams using tabletop rheology and calorimetry. Molecular gels: materials with self-assembled fibrillar networks. 2006:241-52.

23. Aziz ZY, Mohsin MB, Jasim MH. Formulation and Assessment of Delayed/Slow-Release Diclofenac Sodium Edible Organogel Utilizing Low Molecular Weight Organogelators. Iraqi Journal of Pharmaceutical Sciences (P-ISSN 1683-3597 E-ISSN 2521-3512). 2023;32(1):31-9.

24. Fonseca VR, Bhide PJ, Joshi MP. Formulation, development and evaluation of etoricoxib nanosize microemulsion based gel for topical drug delivery. Indian J Pharm Educ Res. 2019;53(4s).

25. Mao K-L, Fan Z-L, Yuan J-D, Chen P-P, Yang J-J, Xu J, et al. Skin-penetrating polymeric nanoparticles incorporated in silk fibroin hydrogel for topical delivery of curcumin to improve its therapeutic effect on psoriasis mouse model. Colloids and Surfaces B: Biointerfaces. 2017;160:704-14.

26. Klein S. Influence of different test parameters on in vitro drug release from topical diclofenac formulations in a vertical diffusion cell setup. Die Pharmazie-An International Journal of Pharmaceutical Sciences. 2013;68(7):565-71.

27. Shahani K, Panyam J. Highly loaded, sustained-release microparticles of curcumin for chemoprevention. Journal of pharmaceutical sciences. 2011;100(7):2599-609.

28. Mohamed MI. Optimization of chlorphenesin emulgel formulation. The AAPS journal. 2004;6:81-7.

29. Singh AR, Kalirajan K. Anti-microbial activity of turmeric natural dyeagainst different bacterial strains. Journal of Applied Pharmaceutical Science. 2012(Issue):210-2.

30. Kali A, Bhuvaneshwar D, Charles PM, Seetha KS. Antibacterial synergy of curcumin with antibiotics against biofilm producing clinical bacterial isolates. Journal of basic and clinical pharmacy. 2016;7(3):93.

31. Alves TMdA, Silva AF, Brandão M, Grandi TSM, Smânia EdFA, Smânia Júnior A, et al. Biological screening of Brazilian medicinal plants. Memórias do Instituto Oswaldo Cruz. 2000;95:367-73.

32. Laupheimer M, Preisig N, Stubenrauch C. The molecular organogel n-decane/12-hydroxyoctadecanoic acid: Sol–gel transition, rheology, and microstructure. Colloids and Surfaces A: Physicochemical and Engineering Aspects. 2015;469:315-25.

33. Amrutiya N, Bajaj A, Madan M. Development of microsponges for topical delivery of mupirocin. Aaps Pharmscitech. 2009;10:402-9.

34. Oxley JA, Ellis CF, McBride EA, McCormick WD. A survey of rabbit handling methods within the United Kingdom and the Republic of Ireland. Journal of Applied Animal Welfare Science. 2019;22(3):207-18.

35. Kim MJ, Park SC, Choi S-O. Dual-nozzle spray deposition process for improving the stability of proteins in polymer microneedles. Rsc Advances. 2017;7(87):55350-9.

36. Fang J-Y, Hung C-F, Chiu H-C, Wang J-J, Chan T-F. Efficacy and irritancy of enhancers on the in-vitro and in-vivo percutaneous absorption of curcumin. Journal of pharmacy and pharmacology. 2003;55(5):593-601.

37. Zhang Y, Xia Q, Li Y, He Z, Li Z, Guo T, et al. CD44 assists the topical anti-psoriatic efficacy of curcumin-loaded hyaluronan-modified ethosomes: A new strategy for clustering drug in inflammatory skin. Theranostics. 2019;9(1):48.

38. Patra D, Barakat C. Synchronous fluorescence spectroscopic study of solvatochromic curcumin dye. Spectrochimica Acta Part A: Molecular and Biomolecular Spectroscopy. 2011;79(5):1034-41.

39. Nawaz A, Wong TW. Microwave as skin permeation enhancer for transdermal drug delivery of chitosan-5-fluorouracil nanoparticles. Carbohydrate polymers. 2017;157:906-19.

40. Hiserodt R, Hartman TG, Ho C-T, Rosen RT. Characterization of powdered turmeric by liquid chromatography-mass spectrometry and gas chromatography-mass spectrometry. Journal of Chromatography A. 1996;740(1):51-63.

41. Yan Y-D, Kim JA, Kwak MK, Yoo BK, Yong CS, Choi H-G. Enhanced oral bioavailability of curcumin via a solid lipid-based self-emulsifying drug delivery system using a spray-drying technique. Biological and Pharmaceutical Bulletin. 2011;34(8):1179-86.

42. Esposito CL, Tardif V, Sarrazin M, Kirilov P, Roullin VG. Preparation and characterization of 12-HSA-based organogels as injectable implants for the controlled delivery of hydrophilic and lipophilic therapeutic agents. Materials Science and Engineering: C. 2020;114:110999.

43. Rogers MA, Wright AJ, Marangoni AG. Engineering the oil binding capacity and crystallinity of self-assembled fibrillar networks of 12-hydroxystearic acid in edible oils. Soft Matter. 2008;4(7):1483-90.

44. Mohamed MBM, Dahabiyeh LA, Sahib MN. Design and evaluation of molecular organogel based on folic acid as a potential green drug carrier for oral route. Drug Development and Industrial Pharmacy. 2022;48(8):367-73.

45. Agrawal V, Gupta V, Ramteke S, Trivedi P. Preparation and evaluation of tubular micelles of pluronic lecithin organogel for transdermal delivery of sumatriptan. Aaps PharmSciTech. 2010;11(4):1718-25.

46. Dantas MGB, Reis SAGB, Damasceno CMD, Rolim LA, Rolim-Neto PJ, Carvalho FO, et al. Development and evaluation of stability of a gel formulation containing the monoterpene borneol. The Scientific World Journal. 2016;2016.

47. Tebcharani L, Wanzke C, Lutz TM, Rodon-Fores J, Lieleg O, Boekhoven J. Emulsions of hydrolyzable oils for the zero-order release of hydrophobic drugs. Journal of Controlled Release. 2021;339:498-505.

48. Mohamed MBM, Qaddoori ZS, Hameed GS. Study the Effect of 12-Hydroxyoctadecanoic Acid Concentration on Preparation and Characterization of Floating Organogels using Cinnarizin as Modeling Drug. Iraqi Journal of Pharmaceutical Sciences (P-ISSN 1683-3597 E-ISSN 2521-3512). 2022;31(2):169-76.

49. Alves C, Ribeiro A, Pinto E, Santos J, Soares G. Exploring Z-Tyr-Phe-OH-based hydrogels loaded with curcumin for the development of dressings for wound healing. Journal of Drug Delivery Science and Technology. 2022;73:103484.

50. Sharifi S, Fathi N, Memar MY, Hosseiniyan Khatibi SM, Khalilov R, Negahdari R, et al. Anti-microbial activity of curcumin nanoformulations: New trends and future perspectives. Phytotherapy Research. 2020;34(8):1926-46.

51. Zeng C, Wan Z, Xia H, Zhao H, Guo S. Structure and properties of organogels developed by diosgenin in canola oil. Food Biophysics. 2020;15:452-62.

52. Yan N, Xu Z, Diehn KK, Raghavan SR, Fang Y, Weiss RG. How do liquid mixtures solubilize insoluble gelators? Self-assembly properties of pyrenyl-linker-glucono gelators in tetrahydrofuran–water mixtures. Journal of the American Chemical Society. 2013;135(24):8989-99.

53. Rogers MA, Wright AJ, Marangoni AG. Crystalline stability of self-assembled fibrillar networks of 12-hydroxystearic acid in edible oils. Food Research International. 2008;41(10):1026-34.

54. Raynal M, Bouteiller L. Organogel formation rationalized by Hansen solubility parameters. Chemical communications. 2011;47(29):8271-3.

55. Terech P, Pasquier D, Bordas V, Rossat C. Rheological properties and structural correlations in molecular organogels. Langmuir. 2000;16(10):4485-94.

56. Pelikh O, Pinnapireddy SR, Keck CM. Dermal penetration analysis of curcumin in an ex vivo porcine ear model using epifluorescence microscopy and digital image processing. Skin Pharmacology and Physiology. 2021;34(5):281-99.

57. Nawaz A, Farid A, Safdar M, Latif MS, Ghazanfar S, Akhtar N, et al. Formulation Development and Ex-Vivo Permeability of Curcumin Hydrogels under the Influence of Natural Chemical Enhancers. Gels. 2022;8(6):384.

58. Shah S, Tahir M, Safdar A, Riaz R, Shahzad Y, Rabbani M, et al. Effect of permeation enhancers on the release behavior and permeation kinetics of novel tramadol lotions. Tropical Journal of Pharmaceutical Research. 2013;12(1):27-32.